

Dynamic Wake Analysis of a Wind Turbine Providing Frequency Containment Reserve in High Wind Speeds

Narender Singh^{1,2*}, Jeroen De Koning^{1,3}, Lieven Vandeveldel^{1,2}

¹Department of Electromechanical, Systems and Metal Engineering,
Faculty of Engineering and Architecture, Ghent University, Belgium

²FlandersMake@UGent.be - Corelab EEDT-DC, Flanders Make, Belgium

³FlandersMake@UGent.be - Corelab EEDT-MP, Flanders Make, Belgium

*narender.singh@ugent.be

Keywords: Frequency containment reserve, Wake effect, Frequency based control, Wind turbine control

Abstract

With the continuous evolution of the power system towards a more renewable energy based system, a natural and gradual transition will be to provide ancillary services by using renewable production units. Research has shown this to be feasible for wind farms by using efficient prediction and sophisticated control systems. In some parts of the world, strict grid codes are already being implemented that require wind farms to provide ancillary services. Moreover, the primary reserve market in Europe is moving towards shorter procurement periods, providing wind farms an opportunity to more efficiently optimise their resources based on short term forecasts. As a result of these developments, it is expected that more wind farms will provide ancillary services in the near future. The provision of Frequency Containment Reserve (FCR) requires a fast regulation of the turbine power based on the changes of the grid frequency. It is expected that this will have an impact on the wake behind the wind turbine. In wind parks with a high capacity density, such as the offshore wind parks in Belgium, it is important to investigate this impact as it can affect other neighbouring turbines. This paper investigates the dynamic behaviour of the wake generated by a wind turbine providing grid frequency support with FCR.

1. Introduction

In line with the European Union (EU) target for 2050 to reduce greenhouse gas emissions to 80-95% below the 1990 levels [1], the power systems all over Europe see an increasing renewable energy penetration every year. In 2019, Europe added 15.4 GW of new wind power capacity. This adds up to a total of 205 GW of installed wind energy capacity in Europe. In 2019, 15% of the total electricity consumed by all EU-nations was generated by using wind energy [2].

As the share of wind energy increases in the power mix, it is naturally expected that wind farms provide ancillary services. In some areas of the world, strict grid codes are already being implemented that require wind farms to provide ancillary services [3]. Studies conducted have shown the feasibility of wind farms as FCR provider [4]. An added advantage for wind farms in this scenario is that the FCR market in Europe is moving towards shorter procurement periods [5]. Since the wind prediction is better on short scale, it is easier for wind farms to make a more confident bid in the FCR market.

In order to provide ancillary services with a wind turbine, its power output must vary more dynamically, especially when providing short-term grid balancing services such as inertial response and FCR. However, these dynamic power variations impact the wake effect, which in turn could impact neighbouring turbines. The study of wake effects is even more significant for wind farms with high capacity density. Countries like Belgium and Germany have high capacity densities of offshore wind farms as compared to the European average. The reason for this high density in Belgium is the regulatory framework. Due to the limited space resources in

Belgium, the obligated policy demands the use of space granted as intensively as possible [6].

The wind farms located in close proximity generate wake effects that reduce the downwind wind speeds. Studies have shown that these effects can extend over 50 km resulting in high economic losses for the wind farms owners [7]. Methods have been developed in order to minimise the impact of the wake and optimise the wind farm power output. These methods use algorithms developed to maximise the annual energy production (AEP) of wind farms [8]. One such approach to maximise the power of a wind farm utilises optimised yaw alignment that deflects wakes away from downstream turbines and wind farms [9]. Such measures have shown to improve the wind speed by up to 13%. Studies have been conducted to demonstrate the significance of wake effects in influencing the inertial response capacity of a wind farm [10]. However, a research gap is seen for studies on wake effects produced by wind turbines providing FCR.

To this end, the scope of this paper lies in the study of dynamic wake behaviour of a wind turbine providing FCR. The study presented in this paper uses a detailed wind turbine model to simulate FCR based control. The influence of the control strategy on the wake behind the turbine at several radial and axial locations is observed. The model uses a conventional proportional-integral (PI) controller to generate blade pitch commands. The torque is controlled by a grid frequency following algorithm. A reference power is generated based on the frequency and the power output is adjusted accordingly. Different frequency profiles have been used in the presented simulations, including an actual extreme grid frequency event.

2. Wind turbine model

The simulations presented in this paper are performed in FAST.Farm developed by the National Renewable Energy Laboratory (NREL). FAST.Farm is a mid-fidelity multi-physics engineering tool for predicting the power performance and structural loads of wind turbines within a wind farm. FAST.Farm combines OpenFAST (an open-source wind turbine simulation tool) with newly developed modules that can simulate farm wide control, calculate wake dynamics of individual rotors and process ambient wake interactions across the wind plant.

The wind turbine model used in the simulations is the NREL 5 MW baseline wind turbine. This model has been implemented in FAST by NREL, a tool for simulating the coupled dynamic response of wind turbines. This elaborate software combines aerodynamic, hydrodynamic, structural and electrical system models of different types of wind turbines. The turbine model used here was featured in various versions of FAST and OpenFAST as part of certification tests. The main model properties are listed in Table 1 [11].

Table I Main properties of the simulated wind turbine

Property	Specification
Power rating	5 MW
Rotor orientation, configuration	Upwind, 3 blades
Rotor diameter, Hub diameter	126 m, 3 m
Hub height	90 m
Cut-in, Rated, Cut-out speed	3 m/s, 11.4 m/s, 25 m/s

The wind turbine is a conventional 3-bladed variable speed upwind turbine. The model is largely based on publicly available data on wind turbines such as the Repower 5M machine.

The drivetrain consists of a gearbox and a doubly-fed induction generator, both included in the reference wind turbine model. The main drivetrain properties are presented in Table II. These parameters are based on data from actual wind turbine generators.

Table II Main properties of the generator

Property	Specification
Power rating	5 MW
Rated generator speed	1173.7 rpm
Nominal efficiency	94.4%
Gearbox ratio	97:1
Generator Inertia	534.116 kg.m ²
Shaft brake time constant	0.6 s

3. Data

The simulations presented in this study require two essential datasets. The developed FCR based control model requires a frequency input on every time step. On the other hand, to be

able to run a wind turbine model in FAST.Farm, a fitting wind field model is necessary.

3.1. Frequency

The simulations presented in this work are performed for 2 different frequency profiles. These data form an important input for the controller as it determines the reference power for the frequency following controller. The first frequency dataset is an artificially generated frequency with a sinusoidal ripple, with a period of 250 seconds and an amplitude of 0.2 Hz oscillating around a mean frequency of 50 Hz. Figure 1 shows a sample of these data. The frequency is sampled at the same rate as the time step for simulations, i.e. 0.5 seconds.

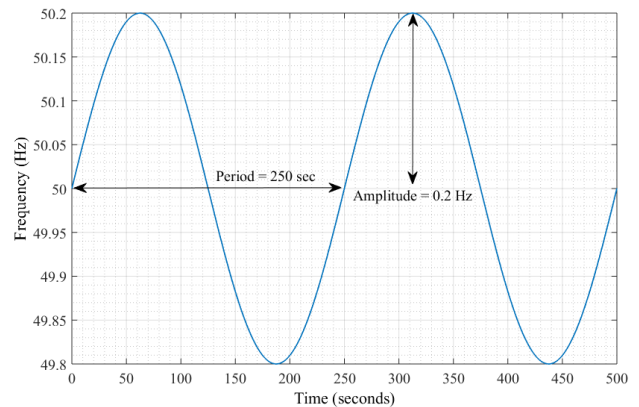


Figure 1 Frequency with sinusoidal ripples

The second frequency dataset is actual grid frequency of the European synchronous grid. The frequency retrieved from the source is sampled every 10 seconds [12]. However, to adjust the frequency to the simulation time-step, one frequency sample is processed every 0.5 seconds. Figure 2 presents a section of frequency data used in the simulations. The frequency data are from an extreme event that occurred on the 10th of January 2019, 21:02 CET. During this event, the continental European power system stretching across 26 countries witnessed the largest absolute frequency deviation since 2006 [13]. During this rare event, the frequency dropped to 49.8 Hz. The reason for choosing this event is to clearly observe the impact of changing grid frequency on a turbine providing FCR.

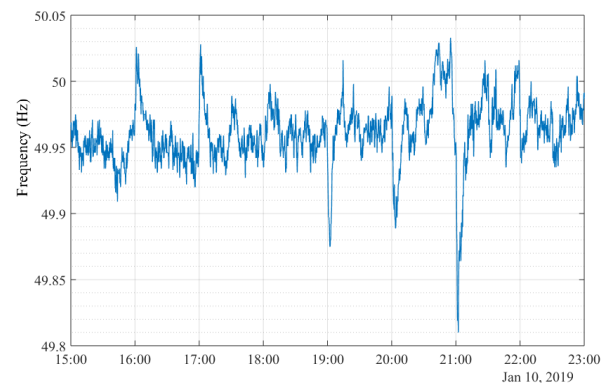


Figure 2 Grid frequency

3.2. Wind field

In FAST.Farm, different wind profile input methods are available and can be used for analysis. One method to input these wind fields is the Inflow wind module. This module is coupled to FAST.Farm through OpenFAST and provides several input options including a steady wind, uniform wind and binary wind files generated by using TurbSim. In the simulations presented in this work, a steady wind profile of 12 m/s is used. The speed is chosen to be above the rated wind speed of the wind turbine so that maximum power is available at all times. Figure 3 shows the simulated wind field and the wake behind the wind turbine. The wind field extends 3000 m in width and 3000 m in length. These dimensions are chosen so that all the points for assessment by FAST.Farm can be encompassed within the wind field. The wind turbine is placed at the centre point with respect to the grid width.

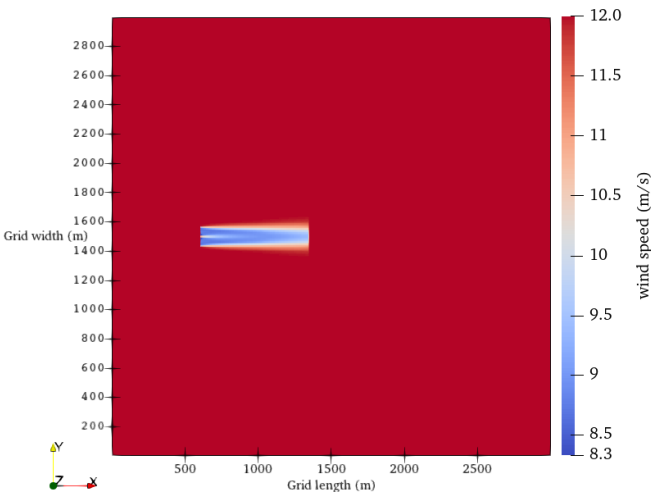


Figure 3 Simulated wind field

4. Control

The conventional operation of a wind turbine is to use maximum power point tracking (MPPT) to extract maximum power or power limiting control (PLC) in case of wind speeds higher than the rated wind speed. FAST.Farm uses its torque and pitch control algorithms to operate in these control modes. However, for our study, we need a control method that can track the grid frequency to provide FCR, instead of tracking the maximum power point.

There are several control options available within FAST.Farm, but there is no existing control method that can include the effect of changing grid frequency on a wind turbine providing FCR. For this reason, the Baseline Control System in FAST.Farm has been modified for this study, to operate the turbine with FCR control. In the Baseline Control System, the power output is controlled through the torque. The operation of the controller is divided into 5 different regions based on the wind speed. These regions are Region 1, Region 1.5, Region 2, Region 2.5 and Region 3. Region 1 is a control region before cut-in wind speed. The torque in this region is zero and no power is extracted from the wind speed. Region 1.5 is as a start-up region and serves as a linear transition between Region 1 and 2. In Region 2 power capture

is optimised. The generator torque in this region is proportional to the square of filtered generator speed. Region 2.5 serves as a linear transition between Region 2 and 3. Region 3 operation is active for wind speeds above the nominal value of 11.4 m/s. The generator power is held constant in this region. The simulations presented in this study are in Region 3 of operation. The operation is modified such that instead of providing a constant power, the power output is based on the changing input grid frequency.

The Belgian TSO Elia procures grid frequency balancing services through two different frameworks based on the generation capacity of the production units. These contracts are the Contract for the Injection of Production Units (CIPU) and non-CIPU. At the moment there are several symmetrical and asymmetrical services. However, for harmonisation of FCR products and FCR procurement rules on the European level, from July 2020 on, only the 200 mHz symmetrical service will be continued [15]. Due to this reason, the tests presented in this work are conducted for a 200 mHz symmetrical service. In this type of service, a proportional frequency support within the range of 49.8-50.2 Hz of grid frequency is required from the participating production unit.

The wind turbine model used in the simulations has a nominal power of 5 MW. In order to provide 1 MW of FCR, the wind turbine is operated at a base power of 4 MW. The turbine ramps up and down within the range of 3-5 MW based on the changing grid frequency. In this manner, there is enough capacity at all times to follow the grid frequency in the specified range. For implementation of this control strategy it is essential that the wind speed is always above the rated wind speed of the wind turbine, 11.4 m/s. Hence, a steady wind speed of 12 m/s is chosen for simulations.

The control function to generate the reference power is defined in (1).

$$P_{\text{ref}} = 4 \text{ MW} + P_{\text{freq}}(t) \quad (1)$$

Here, P_{ref} is the reference power and P_{freq} is the frequency based power margin, that ranges between -1 MW and +1 MW, and is proportional to the deviation of the grid frequency from its nominal 50 Hz.

The relation between the reference power and the grid frequency for a 200 mHz symmetrical service can be seen in Figure 4. In this representation, the wind turbine operates at a base power of 4 MW. With the change in grid frequency, the reference power follows a linear slope between 3 MW and 5 MW. The service is obligated between the bounds of 49.8 Hz – 50.2 Hz. However unlikely, if the frequency drops or increases beyond this range, the power supply should be maintained at a constant, on upper or lower limit respectively. A frequency response deadband of 10 mHz centred at nominal frequency (50 Hz) is present to reduce excessive controller activities and turbine mechanical wear for normal power system frequency variations.

Figure 5 shows the generator power under PLC and FCR based controls. The generated power is plotted on the left Y-axis and the grid frequency on the right Y-axis. The case considered

here has a steady wind speed input of 12 m/s. It can be seen that the power output under PLC control is constant at 5 MW, whereas, with FCR control, the generator power varies with the changing grid frequency. The effect of changing grid frequency can be seen on the power output. The controller works with a high efficiency, following the reference power with a maximum error of 0.0672 %.

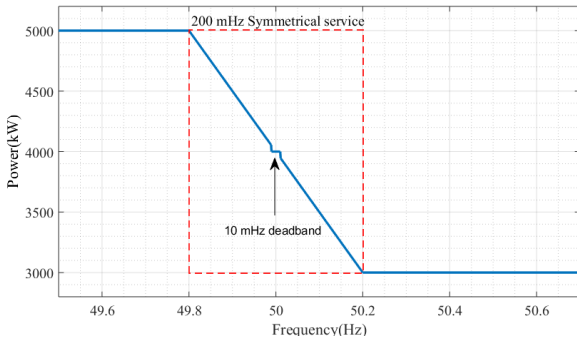


Figure 4 Reference power based on frequency

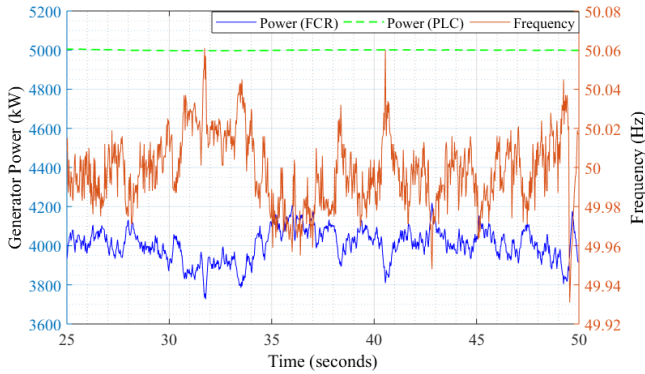


Figure 5 Generator PLC and FCR power

Since the wind turbine operates at a wind speed above the rated wind speed, a pitch control is required. The baseline blade-pitch controller has been used for this purpose. The controller is activated in the region of control where the wind speed exceeds the rated wind speed. The commands from this controller are computed by using gain scheduling PI control on the speed error between the generator speed and the rated generator speed [11].

5. Tests

The tests are divided into two cases based on the frequency data used for control. This division is made to assess the wake effect dynamics in both cases.

5.1. CASE I: Frequency with sinusoidal ripples

In this case, the wind turbine is subjected to a steady wind field of 12 m/s. A frequency with sinusoidal ripples as presented in Section 3 has been used for this simulation. Moreover, to analyse the wake behaviour, 3 different points behind the rotor are chosen at the centreline of the turbine rotor. These points are at distances 373 m, 499 m and 625 m behind the rotor are represented as D1, D2 and D3 respectively in Figure 6.

A steady state section of the simulation is presented in Figure 6. The wind speeds at the specified points can be seen in the figure along with the frequency. Point D1 being closest to the rotor experiences the highest wake effect which results in a lower wind speed. The wind speed gradually increases from point D1 to D3 as the distances from rotor increase. It can also be observed that wind velocity replicates the oscillations of the input frequency. However, a delay can be seen due the distance between the rotor and the specified point.

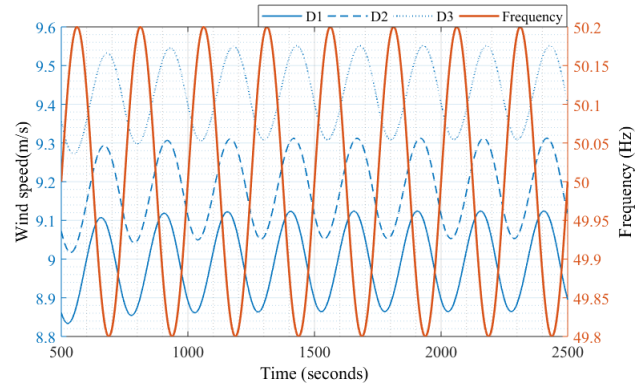


Figure 6 Wind speed behind the rotor at 3 different points

To study the behaviour of the wake at different altitudes behind the turbine rotor, the wind speed is observed at different heights at a distance of 373 m behind the rotor. The different height points begin at the centreline at 90 m altitude and extend up to 150 m with an interval of 15 m. Figure 7 shows the wind speed at these points for a section in steady state of the simulation. The wind speed follows the sinusoidal pattern of the input frequency. The impact of the wake changes at different points in height. The maximum impact is seen at the centreline, where the wind velocity oscillates around a mean speed of 8.9933 m/s. A gradual increase in the wind speed (or reduced wake effect) is observed with the increasing height. On close observation it can also be seen in Figure 7, that the impact of the wake is not directly proportional to the height. The difference between mean speeds at $H = 150$ m and $H = 135$ m is 0.8219 m/s whereas, the difference between the mean speeds at $H = 135$ m and $H = 120$ m is only 0.4788 m/s.

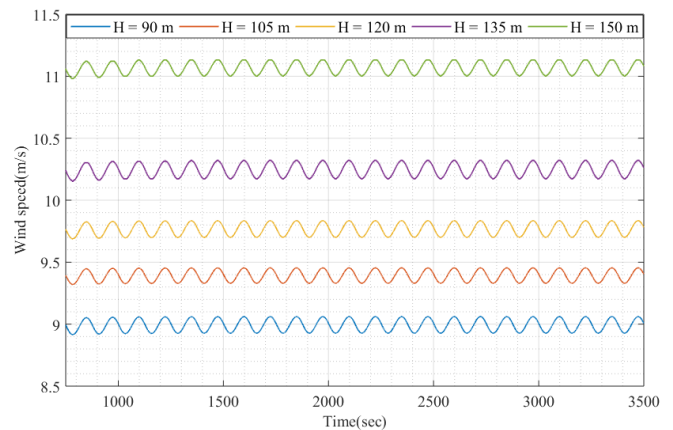


Figure 7 Wind speed at different heights behind the rotor

5.2. CASE II: Real grid Frequency

In this case the wind turbine is subjected to a steady wind of 12 m/s. To simulate a realistic scenario, real grid frequency data are used, as shown in Figure 2. To study the impact on the wake in this case, a point at a distance of 373 m (approximately 3 times the rotor diameter) behind the rotor is chosen at the centreline of the rotor, i.e. a height of 90 m.

Figure 8 presents the plots of grid frequency and the resultant wind speed at the observed point, generator power, torque and generator speed for a section of the simulation. The grid frequency data presented in the figure is a 10 seconds sampled data for 4 hours. However, for computational ease, the simulations are performed on a time-step of 0.5 seconds in FAST.Farm, extracting one frequency data sample every time-step. The data presented in this figure is time aligned with the actual frequency data. An extreme event occurs at time 21:02. At this time the grid frequency suddenly drops to 49.8 Hz. As a result of frequency based control action, the generator power and torque show a corresponding rise as per the 200 mHz service slope, with the power output reaching close to its upper limit of 5000 kW. A change in generator speed is also observed at this time. Due to the control action, a changing wind speed at the point of observation is noticed. This change in the wind speed due to the wake behaviour although clearly noticeable, is rather minimal.

6. Conclusion

To study the behaviour of the wake behind an FCR providing wind turbine, a series of tests are simulated. The control system developed for these simulations regulates the power output through the torque. The torque itself is computed based on the changing input grid frequency. In order to simulate a

realistic scenario, simulations are also performed for actual grid frequency. Moreover, a standard 200 mHz symmetrical FCR service as formed by the Belgian TSO, Elia has been used as a template for these simulations. The controller operates with a high efficiency in tracking the input frequency.

The wake effect has been analysed at several radial and axial points downwind of the wind turbine. The impact of changing grid frequency on the nature of wake is evident. The oscillations in the grid frequency are seen to replicate in the wake behaviour. Also, changes in the intensity of this effect are clearly visible with the changing altitude and distance behind the wind turbine. The changing wake effect can be seen through these observations. However, for this case of single wind turbine operation, this effect is not very high. Even for an extreme drop in grid frequency, only a slight variation in wind speed behind the rotor is observed as compared to the actual wind speed. It can be concluded that the dynamic impact of changing grid frequency on the wake developed by a single standing 5 MW wind turbine is minimal. However, this effect is likely to increase in a high capacity density wind farm where a collective wake effect is generated by several wind turbines.

7. Acknowledgment

This work is supported by the BEOWIND project, funded by the Energy Transition Fund of the Belgian federal government and the FWO research project G.0D93.16N, funded by the Research Foundation Flanders.

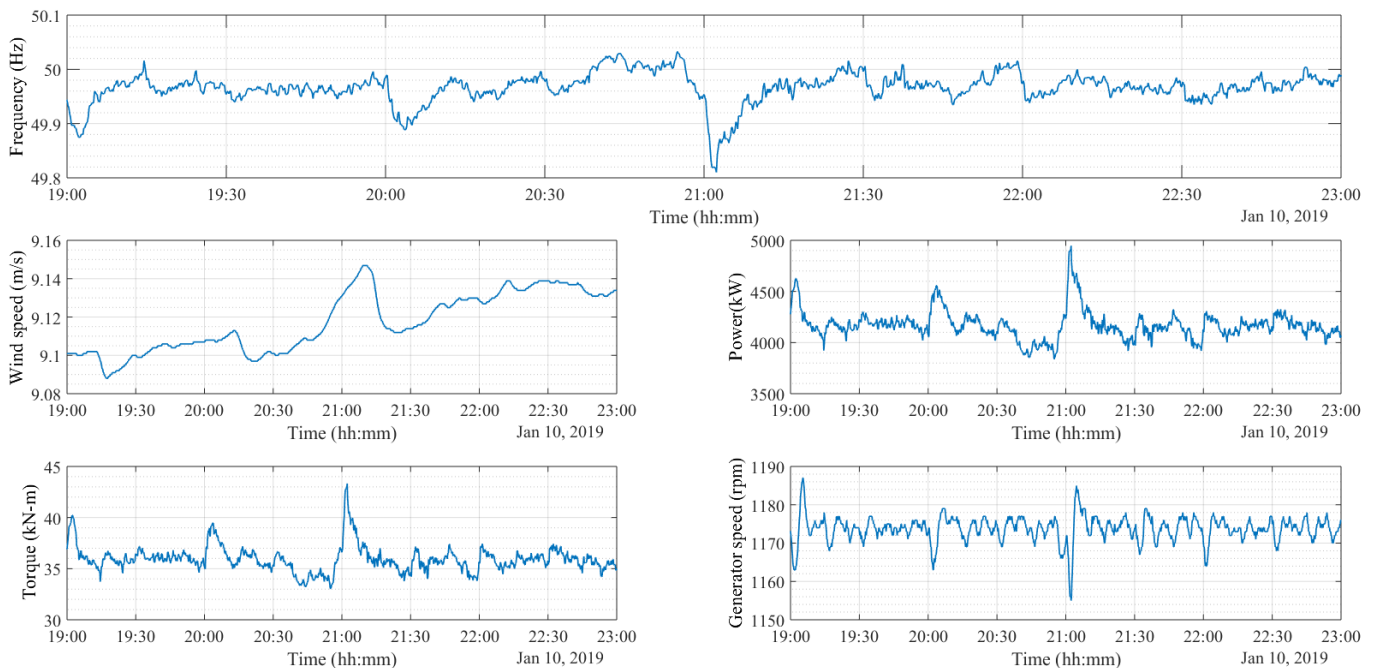


Figure 8 Grid frequency and outputs with changing control action

8. References

- [1] Energy roadmap 2050 Energy. (2012). [online] Available at: https://ec.europa.eu/energy/sites/ener/files/documents/2012_energy_roadmap_2050_en_0.pdf.
- [2] Offshore Wind in Europe Key trends and statistics 2019. (2019). <https://windeurope.org/wp-content/uploads/files/about-wind/statistics>. Wind Europe.
- [3] Technical Requirements for the Connection of Generating Stations to the Hydro-Québec Transmission System. (2019). [online] Available at: http://www.hydroquebec.com/transenergie/fr/commerce/pdf/2_Requirements_generating_stations_D-2018-145_2018-11-15.pdf [Accessed 2 May 2020].
- [4] Singh, N., De Kooning, J. D. M. and Vandeveld, L. Simulation of the Primary Frequency Control Pre-Qualification Test for a 5MW Wind Turbine. In: IEEE PES T&D 2020. Accepted.
- [5] Elia, "General Framework for Frequency Containment Reserve Service by Non-CIPU resources.". Online
- [6] Capacity Densities of European Offshore Wind Farms. (2018). <https://vasab.org/document/capacity-densities-of-european-offshore-wind-farms/>. Deutsche WindGuard GmbH.
- [7] Lundquist, J.K., DuVivier, K.K., Kaffine, D. et al. Costs and consequences of wind turbine wake effects arising from uncoordinated wind energy development. *Nat Energy* 4, 26–34 (2019). <https://doi.org/10.1038/s41560-018-0281-2>
- [8] Baker, N., Stanley, A., Thomas, J., Ning, A. and Dykes, K. (2019). "Best Practices for Wake Model and Optimization Algorithm Selection in Wind Farm Layout Optimization" Preprint. [online] Available at: <https://www.nrel.gov/docs/fy19osti/72935.pdf> [Accessed 2 May 2020].
- [9] Howland, M.F., Lele, S.K. and Dabiri, J.O. (2019). "Wind farm power optimization through wake steering." *Proceedings of the National Academy of Sciences*, [online] 116(29), pp.14495–14500.
- [10] S. Kuenzel, L. Kunjumammed, B. Pal and I. Erlich, "Impact of wakes on wind farm inertial response," 2014 IEEE PES General Meeting | Conference & Exposition, National Harbor, MD, 2014, pp. 1-1.
- [11] Jonkman, J., Butterfield, S., Musial, W. and Scott, G. (2009). "Definition of a 5-MW Reference Wind Turbine for Offshore System Development." [online] Available at: <https://www.nrel.gov/docs/fy09osti/38060.pdf> [Accessed 13 Dec. 2019].
- [12] www.elia.be. (n.d.). Elia: grid data overview. [online] Available at: <https://www.elia.be/en/grid-data> [Accessed 2 May 2020].
- [13] www.entsoe.eu. (n.d.). ENTSO-E technical report on the January 2019 significant frequency deviations in Continental Europe. [online] Available at: <https://www.entsoe.eu/news/2019/05/28/entso-e-technical-report-on-the-january-2019-significant-frequency-deviations-in-continental-europe/> [Accessed 2 May 2020].
- [15] Elia, 2019. General Framework For Frequency Containment Reserve Service By CIPU Technical Units.